

# Soil/Rock Threshold of Colluvial-Deluvial Soil-rock Mixture Based on Numerical Experiment

**Shu Zhang**

*Faculty of Engineering, China University of Geosciences (Wuhan), Wuhan  
430074, P.R.China  
e-mail: [suzy923@foxmail.com](mailto:suzy923@foxmail.com)*

**Li Jiang**

*Architecture & Municipal Department, Central Southern China Electric Power  
Design Institute of China Power Engineering Consulting Group,  
Wuhan 430071, P.R.China  
e-mail: [leonjiang715@sina.com](mailto:leonjiang715@sina.com)*

## ABSTRACT

Soil/rock threshold determination is of great importance in study on physical and mechanical characterization of soil-rock mixture since the value differentiates the stronger blocks from the pervasively fine-grained weaker matrix. This study aimed at determining the soil/rock threshold from both the size distributional and mechanical perspective for the colluvial-deluvial soil/rock mixture, which is distributed ubiquitous in debris landslides of Three Gorges Reservoir Area in China. The soil/rock threshold was analyzed and assumed based on the block grain size distribution based on image process data, as well as the numerical mechanical and hydraulic experiments verification analysis of different specimen dimensions and given soil/rock thresholds. The censored hydraulic and mechanical parameters including unconfined compression strength, Young's modulus, shear strength and hydraulic conductivity. The results indicated that the soil-rock threshold has significant influence to the mechanical and hydraulic properties of colluvial-deluvial soil-rock mixture specimens, especially when the specimens were exerted unconfined compression. The thresholding effect was enhanced under smaller study dimension. Based on comprehensive consideration, the assumption of constant 5mm can be the best adopted threshold in colluvial-deluvial soil-rock mixture for different study dimensions.

**KEYWORDS:** soil-rock mixture; colluvial-deluvial; soil/rock threshold; digital image process; numerical experiment.

## INTRODUCTION

The terminology “soil-rock mixture” is a general expression for those loose deposits in the geological environment composed of a variety of stronger blocks (rock) with different lithologies and sizes embedded in pervasively fine-grained weaker matrix (soil)<sup>[1]</sup>. It is distributed ubiquitous all over the world with various forms of existence, like mélange, agglomerates, breccias, conglomerates, etc. In China this kind of geo-material distributed widely especially in Three Gorges Reservoir Area (TGRA), Qinghai-Tibet Plateau, southwestern mountainous area and southeastern coastal areas. According to different genesis, the thickness various from ten meters to hundreds meters.

Statistical data indicated that 64% of the landslide located in the upstream area of TGRA (1736 totally) was debris landslide<sup>[2]</sup>. Moreover, colluvial-deluvial soil-rock mixture (CDSRM) is considered the main composition of debris landslide in TGRA. Various sizes of blocks distributed in matrix extremely disordered without certain tectonic process, which can be named extremely heterogeneity. The characterization of heterogeneity is the important and difficult points in CDSRM research.

CDSRM, the elfevident is to be composed of block fragments and matrix soils experienced colluviation and deluviation. The matrix soil is a relative concept, which is different from the conventional specific fine soil concepts, like silt or clay<sup>[3]</sup>. The dimension range can be determined by the soil/rock threshold. If the dimension of grain particle is lower than this threshold, the grain can be regarded as matrix soil, otherwise as block. Therefore, the problem of differentiate the blocks from matrix soil (soil/rock thresholding problem) is a key point in calculating the block proportion and obtaining the block dimension distribution. On the consideration of function, the threshold selection has two aspects of demands. Firstly, the portion of block fragments divided into the category of matrix should not affect the physical and mechanical properties of overall. Secondary, the threshold should be selected to the greatest extent, so that avoid meaningless researches.

There have been two different views of soil/rock threshold in the present studies. One is the relative threshold (5% of engineering characteristic dimension,  $0.05L_c$ ) proposed by Medley<sup>[4]</sup>. Medley indicated that mélange in California possessed the characterization of self-similarity and scale-independence, which meant the sizes of block fragments increased with the engineering characteristic dimension. Many researchers adopted this method in soil-rock mixture studying<sup>[3,5-8]</sup>. Another view is the constant dividing line of granule size. For instance, many researches determined 5mm as the threshold<sup>[9,10]</sup>. However, both of the two point of views were proposed based on the granule size distribution. There was no comparison study available as far as we know. Moreover, there was few research verified the threshold from the physical and mechanical aspects because the difficulty in laboratory and field experiments.

The objective of this study was the CDSRM distributed in a typical debris landslide. Firstly, 2D image photographed from the typical CDSRM outcrops were processed and analyzed to extract the meso-structural characteristics. Then generate surrogate models according to the typical outcrops with different soil/rock threshold for numerical physical and mechanical experiments. The simulated results can be compared to analyze the influence of threshold to physical and mechanical properties, so that the most rational soil/rock threshold can be determined.

## OVERVIEW OF STUDYING SITE

Baishuihe landslide, a typical debris landslide in TGRA was selected as the studying site of this research. It is located in Zigui County, Yichang City, Hubei province of China (Figure 1). This landslide site is on the south bank of the Yangtze River, 56 km west of the Three Gorges Dam. The landslide covers an area of  $0.42 \text{ km}^2$  with an estimated volume of  $12,600 \text{ m}^3$ . The fan-shaped landslide extends from an elevation of 75 m to 410 m above mean sea level. According to the newest exploration data, the matrix soil in site is mainly silty clay, and the rock fragments are mainly gray argillaceous siltstones with various dimension. Five drilling holes logs and typical recovered drilled cores illustrated that the thickness of the SRM varied from 3 m to 25 m, with thinner in back edge, and thicker in the front. Our field investigation and the drilled cores also indicated that the maximum observed dimension of the blocks in the mixture was mainly within the range of 20-200 mm, with a few blocks close to 300-500 mm in dimension.

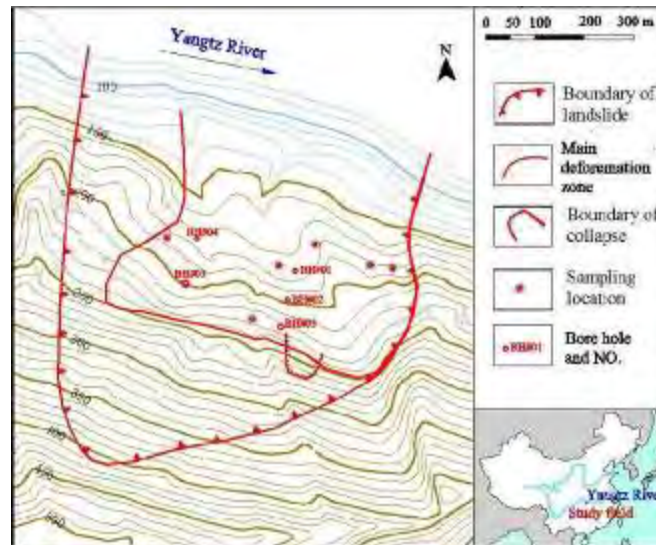


**Figure 1:** schematic plan of Baishuihe landslide and sampling location

Appropriate photographic sampling provided the baseline data for further study. We only selected six outcrops (the sampling location noted in Figure 1) in this region because most of the area were covered by thick vegetation and was inaccessible. The actual dimension of the sampled photos lied between 1.2 m to 2 m because of the dimensional restriction of accessible outcrops. According to the field investigation and drilled cores, all the photographing outcrops can be regarded as representative samples of the site.

## 2D IMAGE PROCESS AND BLOCK CHARACTERIZATION EXTRACTION

### Digital image process and mesostructure extraction

The technology of 2D image process has been applied in complex mixed geo-materials in order to obtain grain mesostructures extensively<sup>[5-6,8,10-12]</sup>. Theoretical and practical analysis indicated that the technology tend to underestimate the real dimension of blocks and thus produce a certain deviation of the block proportion and grain size distribution<sup>[13,14]</sup>. Despite of the intrinsic disadvantages, it is simple, convenient and less consumed in obtain the grain size distribution. Moreover, it could provide mesostructural characteristics of the blocks which cannot be obtained from the conventional 1D scanline observations and 3D sieving tests<sup>[11]</sup>.

The 2D image process in this study was performed using the open image processing program ImageJ. The original outcrop photographs were transformed into binary images after preprocessing. The blocks in the binary image were then segmented and extracted for further analysis. The geometry of blocks is complex, and generally be describe as ellipses or polygons. In this study, we aimed at extracting the mesostructures of block inclusions, thus we simplified the original block geometry into ellipses with 3 elements. As shown in Figure 2, the elements involve maximum observed dimension (MOD), oriental angle (OA), and aspect ratio (AR). MOD refers to the length of the longer axis of the equivalent 2D ellipse. AR is a dimensionless parameter that refers to the elongation of the block, and it is defined as the ratio of the major axis to the minor axis of the fitting ellipse. OA is defined as the angle from the vertical axis to the longest axis

counterclockwise. Thus the value of OA would be from  $0^\circ$  to  $180^\circ$ . The binarization processed image and the simplified surrogate elliptical models can be exhibited in Figure 3 as well.

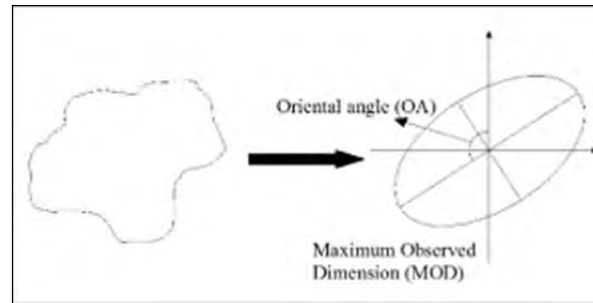
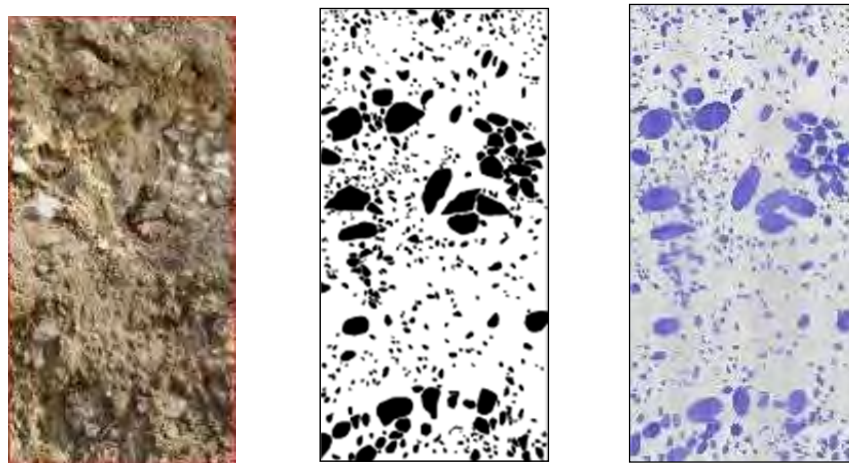


**Figure 2:** Sketch of the fitting ellipse of original block



a. outcrop photograph    b. binarization processed image    c. simplified surrogate model

**Figure 3:** Original outcrop photograph, binarization processed image and simplified surrogate model of CDSRM

### Grain size distribution of censored CDSRM

This study censored the meso-structures extracted from 6 typical CDSRM outcrops. To get a better understanding of the influence of various soil/rock thresholds onto the grain size distribution, we gave 5 certain specific thresholds to verify the proportions of the grain size lower than the given thresholds. The verified soil/rock threshold including: (1) 5mm; (2) 10mm; (3) 5% of the engineering characteristic dimension, i.e.  $0.05L_c$ ; (4) 5% of the maximum grain dimension in the study dimension, i.e.  $0.05d_{max}$ ; (5)  $0.1d_{max}$ .

We utilized normalized block area ratio (ratio of block area to the image sample area) to analyze because the photograph samples did not possess the same dimension. There were 2458 blocks we censored in this study. The accumulative percentage of total block counts and total block area were shown in Figure 4. The results indicated that the minimum MOD of censored blocks was 2.18mm, while the maximum MOD was 529.26mm. Moreover, the percentage of blocks smaller than 5mm was 1.18% of the total block counts, and 0.23% of the total area; while

the percentage of blocks smaller than 10mm was 14.08% of the total block count, and 2.51% of the total area.

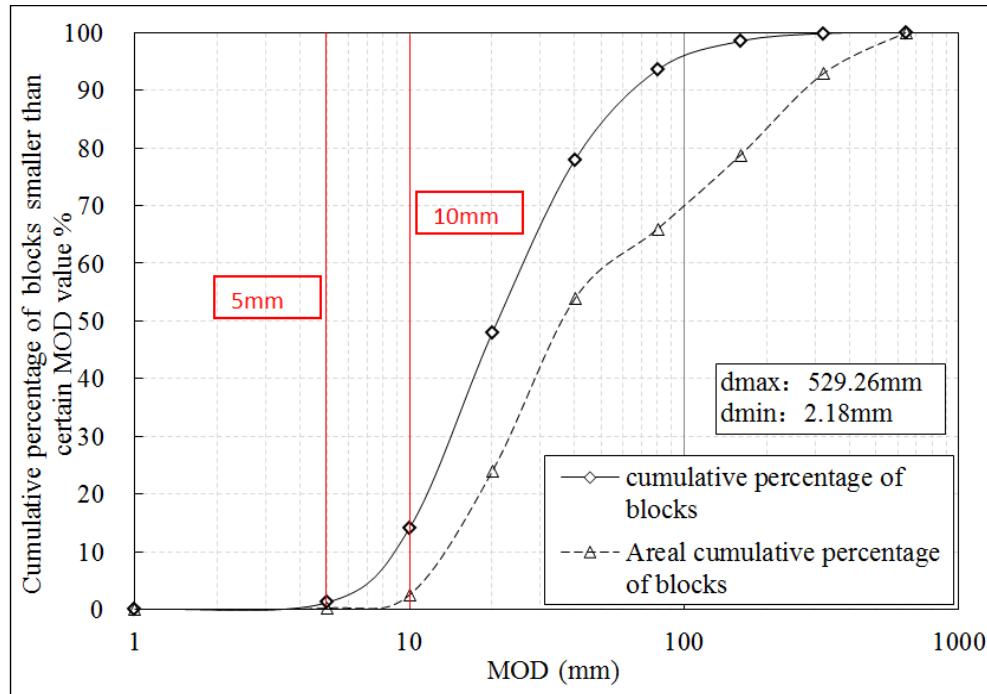


**Figure 4:** Block dimension and corresponding areal cumulative curves

For the sake of censor the relationship of MOD vs  $L_c$  and MOD vs  $d_{max}$ , we plotted the cumulative curves and corresponding areal cumulative curves of the relative block grain dimension (including MOD/ $L_c$  and MOD/ $d_{max}$ ) as well, as shown in Figure 5. The results revealed that the percentage of blocks smaller than  $0.05L_c$  was 89.04% of the total block counts, 60.63% of the total block area and 25.05% of the total outcrop area; while the percentage of blocks smaller than  $0.05d_{max}$  was 33.52% of the total block counts, 0.93% of the total outcrop area and 2.25% of the total block area; the percentage of blocks smaller than  $0.1d_{max}$  was 66.68% of the total block counts, 4.16% of the total block outcrop area and 10.08% of the total area. However, this observation was different from the m $\acute{e}$ lange data censored by Medley, of which the percentage of blocks smaller than  $0.05L_c$  was more than 90% of the total block counts, but less than 1% of the total study area. Therefore, the speculation of neglecting the contribution of these portion (smaller than  $0.05L_c$ ) to the overall mechanical properties and determining  $0.05L_c$  as the soil/rock threshold need to be verify when studying CDSRM, a material not exactly the same as m $\acute{e}$ lange. This study verified the aforementioned 5 various threshold from both the mechanical and hydraulic response of CDSRM outcrop samples using numerical experiments.

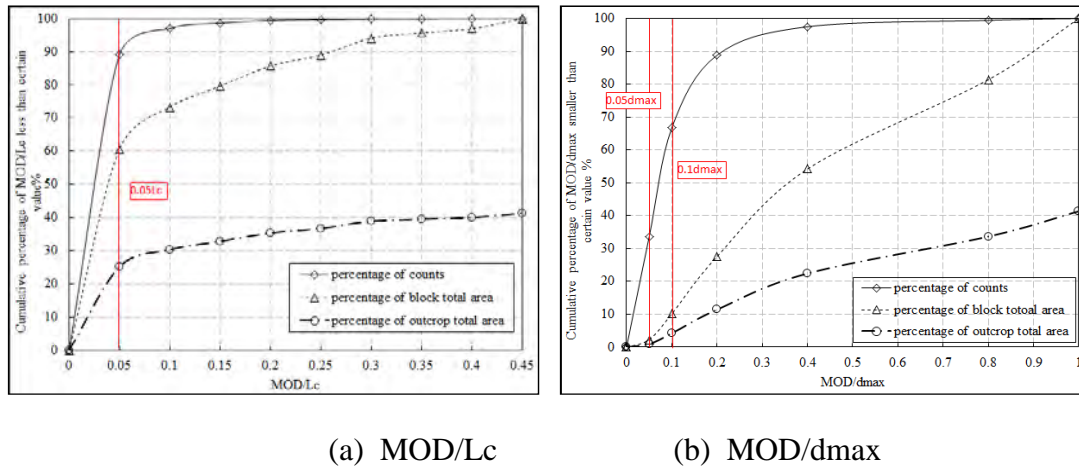


**Figure 5:** Block relative dimension and corresponding areal cumulative curves

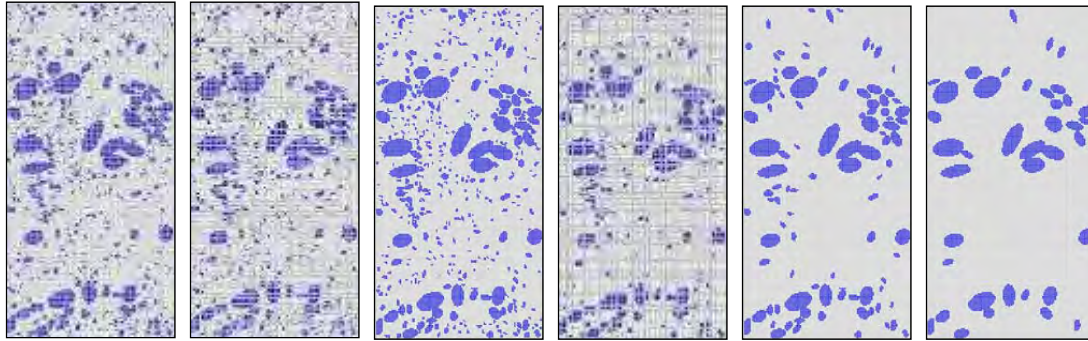
## NUMERICAL MECHANICAL EXPERIMENTS FOR CDSRM

Numerical experiment has been an effective approach when studying the mechanical properties of soil/rock mixture. Although the credibility of determining the mechanical and hydraulic properties using numerical method need to be verified further, it indeed has incomparable advantage in reconstruct the original morphological characteristics and control the block distribution as researcher's demand. The adopted numerical methods involve in finite element method (FEM) [5,8,12], finite difference method (FDM) [15] and discrete element method (DEM) [16,17], etc. The numerical mechanical experiment for CDSRM we adopted in this study was FDM, using FLAC<sup>3D</sup>.

### Generating surrogate model and meshing

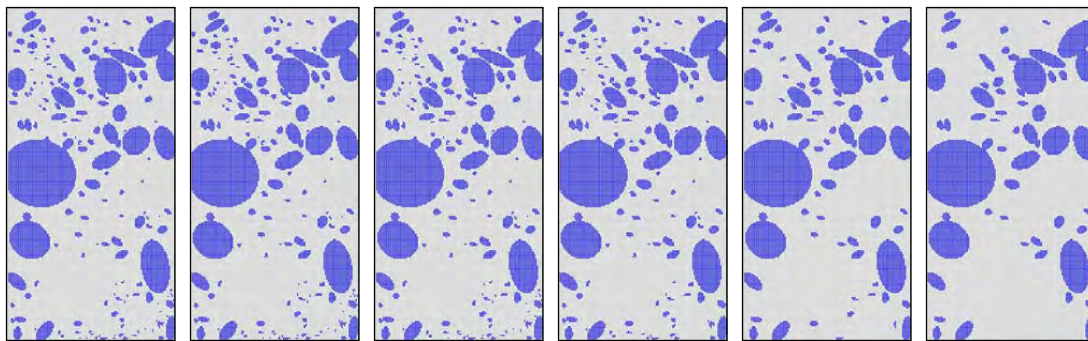
We selected two outcrop photographs with different dimension (300mm×600mm and 600mm×1200mm respectively) as the original specimens. The photographs were processed and extracted the mesostructures as introduced in Figure 2. The surrogate elliptical model were then generated according to the given elliptical elements and threshold. This method was effective when scalping on the basis of given threshold.

The FLAC<sup>3D</sup> (Fast Lagrangian Analysis of Continua in 3 Dimension) reproduced both the pre and post peak behavior of geo-materials [15], and was utilized to perform the numerical experiments in this section. Own-written parametric modeling fish code was produced to generate surrogate models in FLAC<sup>3D</sup>. The size of meshing element was 5mm×5mm×5mm, which is fine enough to reflect the block fragments in surrogate models. Thus the dimensions of the quasi three-dimensional numerical specimens adopted in this study were 300mm×600mm×5mm and 600mm×1200 mm×5mm, respectively. Figure 6 and Figure 7 are the elliptical surrogate models generated in FLAC<sup>3D</sup> according to given soil/rock threshold. The relative small specimen intuitively included more relative small block fragments.



a.original b. 0.05dmax c. 5mm d. 0.1dmax e. 10mm f. 0.05Lc

**Figure 6:** Quasi-three-dimensional specimen with different soil/rock threshold (300mm×600mm)



a.original b. 5mm c. 10mm d. 0.05dmax e. 0.1dmax f. 0.05Lc

**Figure 6:** Quasi-three-dimensional specimen with different soil/rock threshold (600mm×1200mm)

## Loading Approach

We tended to censor the mechanical properties involving in unconfined compression strength, Young's modulus and shear strength, thus numerical unconfined compression test as well as triaxial compression test were performed in this section.

On the aspect of unconfined compression test, the loading approach was exerting constant axial displacement ( $2.5 \times 10^{-6}$ m/time step) from the upper end, and the lower end was fixed, as shown in Figure 7. The axial stress increased with the applying of axial displacement, and produced corresponding deformation until achieved yield limit, which is the unconfined compression strength. We set 9 monitoring points on the different location of specimen to measure the axial displacement. With the knowledge of the cross-section area and the length of the specimen, the stress-strain curve can be computed and plotted. Once stress-strain curve plotted, Young's modulus was determined in term of the tangent modulus of 1/2 yield limit.

With regard to the triaxial compression test, it is actually dual-axial compression test as shown in Figure 7 as well. The applied axial displacement and monitoring method were the same

as that of unconfined compression test. The difference was the lateral stress applying on the lateral sides of the specimen. The lateral stresses we applied in this section were 50KPa, 100KPa, 200KPa and 400KPa, respectively. Mohr-Coulomb criterion was utilized for failure judgement.

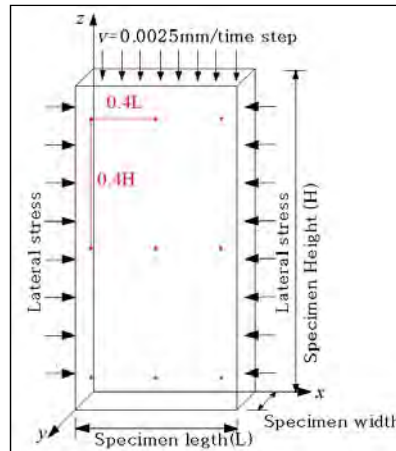


**Figure 7:** Diagrammatic sketch of quasi-three-dimensional specimen dimension, loading regime and displacement monitoring points of numerical experiments

Based on previous studies and empirical experiences of CDSRM in TGRA, the physical parameters of “rock” block and “soil” matrix were defined, as shown in Table 1. The Mohr-Coulomb criterion was adopted as the yield criterion of both the block group element and the matrix group element. The platen effect was not considered, meaning that there was no friction between specimen’s ends and the loading platens. The contacted boundaries between block inclusions and matrix were not considered either.

**Table 1:** Physical and mechanical parameters adopted in the numerical experiments

Component	Density (g/cm <sup>3</sup> )	Elastic modulus (Mpa)	Poisson's ratio	Cohesion (Mpa)	Internal friction angel (°)
Soil	2.0	50	0.3	0.05	28
Rock	2.7	1050	0.2	0.45	38

## NUMERICAL HYDRAULIC EXPERIMENTS FOR CDSRM

Hydraulic conductivity is an important parameter when evaluating the seepage characteristics. Therefore, the censored index in numerical hydraulic experiments was hydraulic conductivity ( $K$ ).

We utilized thermal conductance module of FEM software Abaqus for the hydraulic conductivity simulation. Firstly, it is because thermal conduction equation and Darcy’s steady flow equation share the same mathematical expression, as shown in equation (1):

$$q = -KA \frac{\Delta h}{L} \quad (1)$$

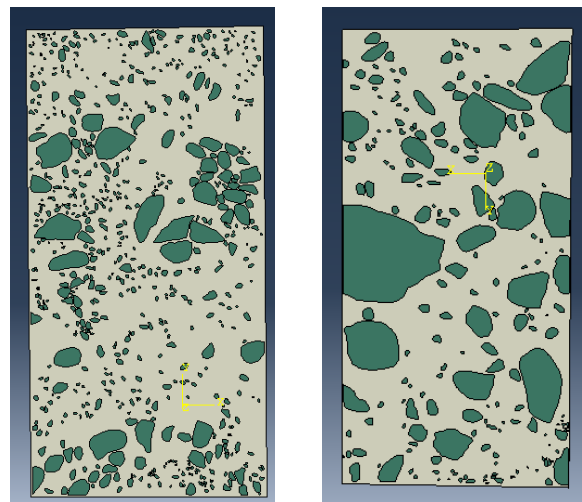


where physical significances of the parameters in thermal conduction equation and Darcy's steady flow equation were shown in Table 2 respectively<sup>[18]</sup>. Accordingly, the seepage problems can be simulated using thermal conductance approach remarkably. Secondary, flow is permitted to propagate both along the normal and tangential direction of the block-soil interface in thermal conductance module. However, flow along tangential direction is not allowed in seepage module.

**Table 2:** Physical significance of parameters

Equation	Parameters				
	$q$	$K$	$\Delta h$	$A$	$L$
Darcy's steady flow equation	Seepage flow	Hydraulic conductivity	Water head difference	Cross-section area	Seepage path length
Thermal conduction equation	Heat flux	Thermal conductivity	Temperature difference	Cross-section area	Heat transfer path length

The simulated CDSRM specimen models were generated in term of given parametric meso-structures as illustrated in aforementioned section other than the extension length along  $z$  axis. We extended 10 mm in this section. Besides, we generated the specimen model according to the original geometry of outcrops for comparison, as shown in Figure 8. We tried to apply hexahedral elements for meshing based on the consideration of element stability. In the case of extremely complex geometry (i.e. specimen models in term of outcrop original geometry), we utilized tetrahedral elements.



(a) 300mm×600mm

(b) 600mm×1200mm

**Figure 8:** Quasi-three-dimensional specimen with different dimension

For the purpose of obtaining the overall hydraulic conductivity of CDSRM, firstly we assigned individual hydraulic conductivity to the matrix soil, block inclusions and block-matrix interface, seen in Table 3. Then we set the temperature (water head) boundary condition on the upper and lower ends. To simplify the calculation, we set temperature (water head) difference the

same as the specimen height, for example, we assigned the temperature (water head) as 0.6 on the upper end of specimen with the dimension of 300mm×600mm, and 0 on the lower end. The flux was calculated using the average flux of the elements of lower end. Then the overall hydraulic conductivity can be evaluated according to equation (1).

**Table 3:** Parameters assigned on the materials

Component	block	matrix	interface
Hydraulic conductivity (m/s)	$5 \times 10^{-8}$	$5 \times 10^{-5}$	$1 \times 10^{-1}$

## RESULTS AND DISCUSSION

We performed 60 sets of numerical unconfined compression tests and triaxial compression tests on the specimen models in total. Figure 9 is the axial stress-strain curves for specimens with various soil/rock threshold of dimension 300mm×600mm. Figure 10 is the axial stress-strain curves of specimen with threshold of 0.05d<sub>max</sub> (3.23 mm) under different lateral stress of dimension 300mm×600mm, as well as the Mohr's stress circles plotted for shear strength indexes. Table 4 and Table 5 are the numerical experiments results for specimens with dimension of 300mm×600mm and 600mm×1200mm, respectively.

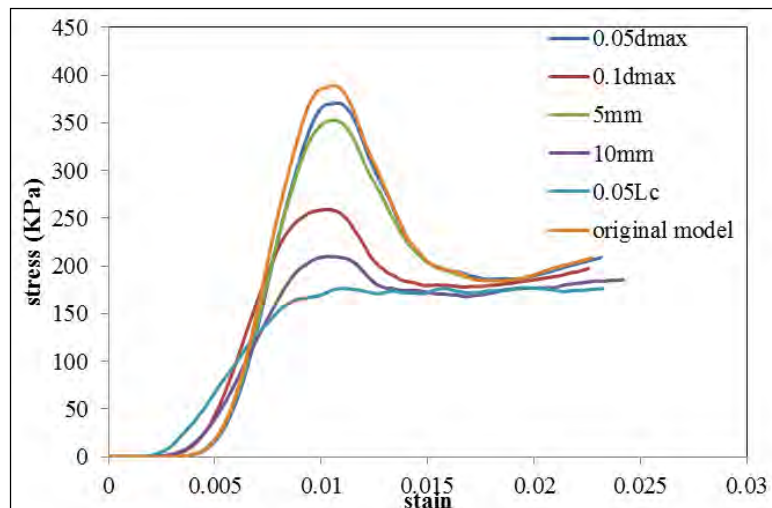


**Figure 9:** Stress-strain curves of numerical unconfined compression test for surrogate specimens with distinct soil/rock threshold (dimension of 300mm×600mm×5mm)  
(Note: stress unit is kPa, not KPa)

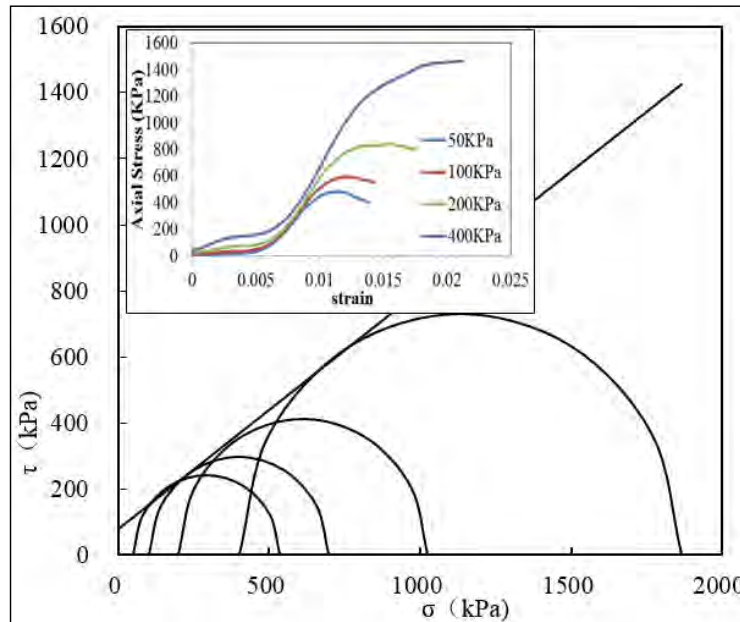


**Figure 10:** Axial stress-strain curves and Mohr's stress circles of numerical tri-axial compression tests for surrogate specimens with 0.05dmax soil/rock threshold (dimension of 300mm×600mm×5mm)

**Table 4:** Numerical mechanical experiment results for specimens with dimension of 300mm×600mm×5mm

300×600	original	0.05dmax	5mm	0.1dmax	10mm	0.05Lc
UCS(KPa)	389.4	370.8	352.8	259.3	210	177.3
E(MPa)	103.2	91.61	76.23	66.02	44.47	30.79
C(KPa)	35.65	35.87	36.33	36.8	36.81	36.24
φ(°)	86	79.4	65.7	54.3	43.2	40.5

**Table 5:** Numerical mechanical experiment results for specimens with dimension of 600mm×1200mm×5mm

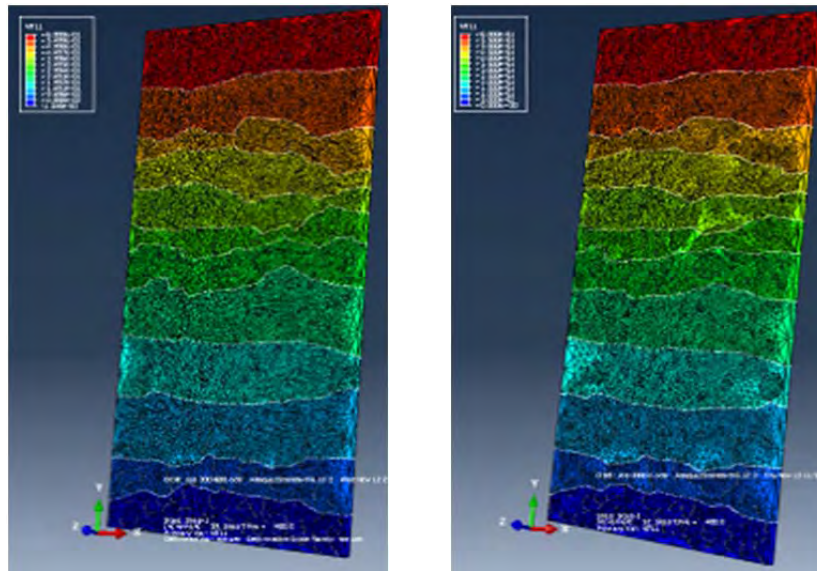
600×1200	original	5mm	10mm	0.05dmax	0.1dmax	0.05Lc
UCS(KPa)	297.8	297.5	297.9	297	278.4	269
E(MPa)	62.59	62.45	61.39	59.34	57.14	55.47
C(KPa)	37.34	37.26	37.37	37.39	37.52	37.14
φ(°)	68.1	68.4	67.6	67.1	64.4	64.1

14 sets of numerical hydraulic experiments were performed as well. For example, Figure 11 is the temperature nephograms of the original geometry specimen and original elliptical surrogate specimen with dimension of 300mm×600mm×5mm. And the calculated overall hydraulic conductivity can be seen in Table 6.

**Table 6:** Calculated overall hydraulic conductivity of specimens (m/s)

Specimen dimension	Original geometry	Original surrogate	0.05dmax	5mm	0.1dmax	10mm	0.05Lc
300×600	3.05E-05	3.11E-05	3.15E-05	3.12E-05	3.33E-05	3.51E-05	4.27E-05
600×1200	2.08E-05	2.19 E-05	2.36 E-05	2.24 E-05	2.43 E-05	2.30 E-05	2.46 E-05

The comparison diagram of the comprehensive numerical experiment results of various soil/rock thresholds are shown in Figure 12. The y axis ( $X_i/X_{ori}$ ) refers to the ratio of thresholded specimen values to the original elliptical surrogated specimen values of the censored mechanical and hydraulic parameters.



(a) original geometry specimen      (b) original elliptical surrogate specimen

**Figure 11:** Temperature nephograms of the original geometry specimen and original elliptical surrogate specimen with dimension of 300mm×600mm×5mm

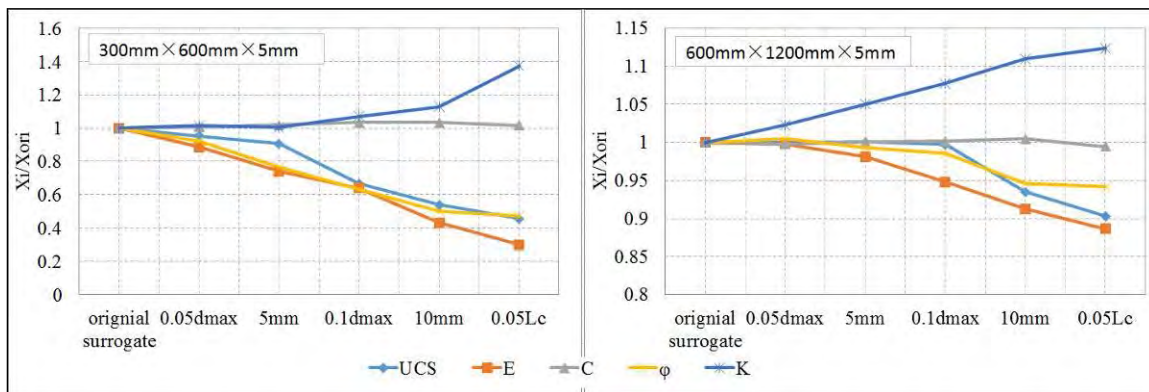


**Figure 12:** Comparison diagram for comprehensive numerical experiment results

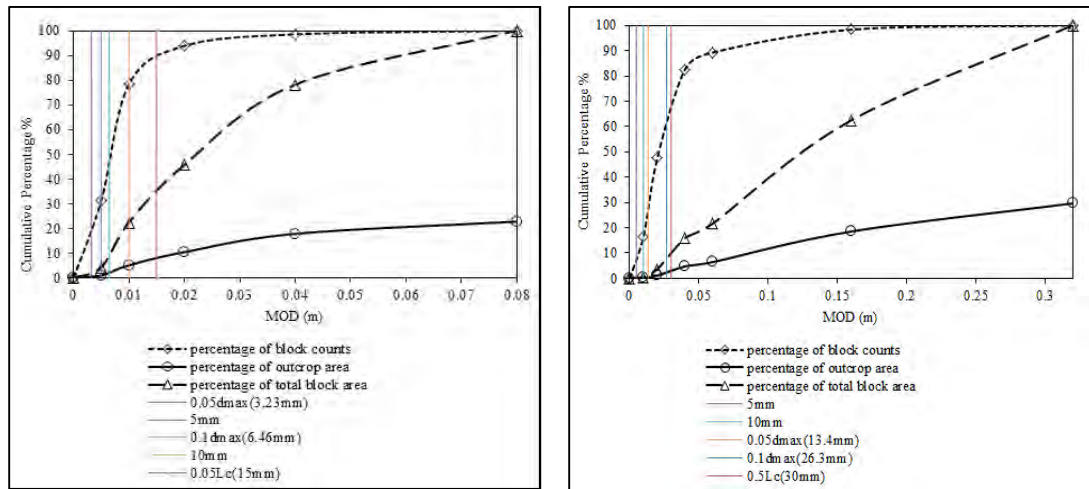
All the above numerical experiments illustrated the following results:

- (1) The unconfined compression strength (UCS) and Young's modulus (E) both decreased with the increase of soil/rock threshold for the two specimen dimensions we considered. On the aspect of shear strength, internal friction angle decreased with the increase of soil/rock threshold, while cohesion stabilized without significant variation. It may be because the extremely heterogeneity of soil-rock mixture arouse significant structure effect of stress field under unconfined compression<sup>[12]</sup>. The structure effect is so remarkable that the commonly undercounted small blocks would give rise to stress concentration, thus affect the UCS and E evaluations. On the contrary, when the specimen was under triaxial compression, the lateral stress would weaken the structure effect relative to unconfined compression test, thus the stress concentration phenomenon also weakened and the variation of shear strength weakened as well.
- (2) The influence of soil/rock threshold to the overall specimen mechanical properties is more significant when the specimen has relative small dimension. For example, the differences of UCS and E for original surrogate specimen and 0.05Lc thresholding specimen with dimension of 300mm×600mm×5mm reach to 212.1 KPa and 72.41 MPa respectively, which is 119.6% and 235.1% of the values of 0.05Lc thresholding specimen's values. On the contrary, the differences are only 28.8 KPa and 7.12 MPa of specimens with dimension of 600mm×1200mm×5mm, which are only the 10.7% and 12.8% of the 0.05Lc thresholding specimen's values. That is, the thresholding effect enhanced on the scenario of smaller specimen size.
- (3) The hydraulic conductivity of elliptical surrogate specimen models is greater than that of original geometric specimen models, which can be explained that the angularity of block surface increases the tortuosity of propagating path of flow, thus decreases the overall hydraulic conductivity. The temperature nephogram of original geometric model exhibited the pattern of more angular (Figure 11), which is another exemplification of the explanation.
- (4) Despite of the angularity influence, the hydraulic conductivity evolution of elliptical surrogate models with various soil/rock thresholds could reflect some general regulation. As shown in Figure 12, with the increase of soil/rock threshold, the hydraulic conductivity increased. The highest increasing rate (37%) appears on the specimen with largest censored threshold (0.05Lc) and smaller dimension. The increasing rates of other specimens are no more than 15%.

We investigated the correlation of block grain distribution and soil/rock thresholding effect as well since the two original outcrop specimens have distinct grain size distribution (Figure 13). The results indicated that the proportion of relative smaller blocks for smaller specimen is greater than that of larger specimen. It is noticed that under the scenario of smaller specimen and 0.1d<sub>max</sub> thresholding, the areal percentage of the undercounted blocks to the total block is less than 10%, which is similar as that all thresholding scenarios of larger specimens. However, the significant reduction of UCS, E and internal friction angle are still existed. Therefore, we can draw the conclusion that thresholding effect is enhanced when specimen has relative small size.

It should be pointed out that larger specimen size could reflect the block size distribution characteristics better than smaller specimen did, which can be exemplified by the cumulative curves comparison of Figure 4 and Figure 13. However, the present dimension of soil-rock mixture specimens were generally limited by the cylinder specimen with diameter of 300 mm and height of 600mm. Consequently, selecting a rational soil/rock threshold becomes remarkably important in this meaning.

Besides, all above numerical experiments results revealed that the commonly adopted soil/rock threshold ( $0.05L_c$ ) tends to produce over-conservative mechanical properties and overlarge hydraulic conductivity. In contrast, from the aspects of block grain size distribution and mechanical (hydraulic) properties, selecting 5 mm or  $0.05d_{max}$  as the thresholding value is more rational. While the  $d_{max}$  is not easily too estimate in practice, thus it is more reasonable that select constant 5mm as the soil/rock threshold for CDSRM.



(a) 300mm×600mm×5mm

(b) 600mm×1200mm×5mm

**Figure 13:** Block cumulative curves and corresponding areal cumulative curves

## CONCLUSIONS

On the consideration of CDSRM and mélangé (bimrock) has distinct grain size distribution characteristics, the commonly adopted soil/rock threshold ( $0.05L_c$ ) may not be reasonable for CDSRM. Therefore, we performed numerical mechanical and hydraulic experiments on the CDSRM outcrop specimens of typical debris landslide in TGRA and corresponding elliptical surrogate specimens with various soil/rock thresholds.

Numerical mechanical experiments results indicated that unconfined compression strength and Young's modulus have a significant reduction effect with increase of soil/rock thresholding. However, this reduction effect is not significant under the condition of triaxial compression tests, of which the internal friction angle has a slight reduction, while cohesion is invariable generally. It may be because the extremely heterogeneity of soil-rock mixture arouse significant structure effect of stress field under unconfined compression. The structure effect is so remarkable that the commonly undercounted small blocks would give rise to stress concentration, thus affect the strength and deformability evaluations. On the contrary, when the specimen was under triaxial compression, the lateral stress would weaken the structure effect, thus the stress concentration phenomenon and the variation of shear strength weakened as well. Besides, numerical hydraulic experiments results indicated that hydraulic conductivity has a slight enhancement effect with increase of soil/rock thresholding. All the thresholding effect are relative remarkable in the smaller specimen.

All the numerical experiments results revealed that the commonly adopted soil/rock threshold (0.05Lc) tends to produce over-conservative mechanical properties and overlarge hydraulic conductivity. In contrast, from the aspects of block grain size distribution and mechanical (hydraulic) properties, selecting 5 mm or 0.05d<sub>max</sub> as the thresholding value is more rational. While the d<sub>max</sub> is not easily too estimate in practice, thus it is more reasonable that select constant 5mm as the soil/rock threshold for CDSRM.

## ACKNOWLEDGEMENT

The idea of present work was mainly figured out while the author visiting Department of Geology and Geophysics, Texas A&M University, USA. The author gratefully acknowledge Professor Huiming Tang's research group at the China University of Geosciences (Wuhan) for providing the original data used in this study.

## REFERENCES

1. W., Xu, R., Hu, and R., Tan (2007) "Some geomechanical properties of soil-rock mixtures in the Hutiao Gorge area, China," *Geotechnique*, Vol 3: pp 255-64.
2. Jinwu, Xia and Houzhen, Guo (1997) "Investigation of landslide distribution characterization and main control factor of Changjiang upstream area," *Hydrogeology and Engineering Geology*, No.1, pp 19-22. (in Chinese)
3. Wenjie, Xu and Ruilin, Hu (2009) "Conception, classification and significations of soil-rock mixture," *Hydrogeology and Engineering Geology*, No.4, pp50-56. (in Chinese)
4. Medley, E.W. (1994) "The engineering characterization of mélanges and similar block-in-matrix rocks (bimrocks)," University of California, Berkeley. (Ph.D. dissertation)
5. Wenjie, Xu, Zhongqi, Yue and Ruilin, Hu (2008) "Study on the Mesostructure and Mesomechanical Characteristics of the Soil-rock Mixture Using Digital Image Processing Based Finite Element Method," *International Journal of Rock Mechanics & Mining Sciences*, Vol 45, pp 749-762.
6. Wenjie, Xu and Qiang Xu (2012) "Study of quantitative description method of geomaterial meso-structure ——taking soil rock mixture for example," *Chinese Journal of Rock Mechanics and Engineering*, Vol 31, No.3, pp499-506. (in Chinese)
7. Zhongqiang, Liu, Yadong, Xue, Hongwei, Huang, et al. (2012) "Experimental research on shear behavior of colluvium," *Rock and Soil Mechanics*, Vol 33, No. 8, pp 2349-2358. (in Chinese)
8. ZQ, Yue, S, Chen, LG, Tham (2003) "Finite element modeling of geomaterials using digital image processing," *Computers and Geotechnics*, Vol 30, pp75-397.
9. Yun, Dong and Hejun, Chai (2007) "Study on engineering synthetical classification of rock-soil aggregate mixture," *Rock and Soil Mechanics*, Vol 28, No. 1, pp 180-184. (in Chinese)
10. Anquan, Xu, Weiya, Xu, Chong, Shi, et al. (2012) "Micromechanical properties and mechanical parameters of talus deposit based on digital image technology," *Chinese Journal of Rock Mechanics and Engineering*, Vol 34, No. 1, pp58-64. (in Chinese)

11. Coli, N., Berry, P., Boldni, D. (2012) "The contribution of geostatistics to the characterisation of some bimrock properties," *Engineering geology*, Vol 137, pp 53-63.
12. Qiulin, Liao, Xiao, Li, Wangcheng, Zhu (2010) "Structure model construction of rock and soil aggregate based on digital image technology and its numerical simulation on mechanical structure effects," *Chinese Journal of Rock Mechanics and Engineering*, Vol 29, No.1, pp155-162. (in Chinese)
13. WC, Haneberg (2004) "Simulation of 3D block populations to characterize outcrop sampling bias in bimrocks," *Felsbau*, Vol 22, No.5, pp 19-26.
14. EW, Medley (1997) "Uncertainty in Estimates of Block Volumetric Proportions in Melange Bimrock," *Proceedings International Symposium on Engineering Geology and the Environment*, Athens, pp 267-272.
15. YW, Pan, MH, Hsieh, MH, Liao (2008) "Mechanical Properties of virtual block-in-matrix colluvium," *Proceedings of American Rock Mechanics Association*, San Francisco, pp 8-16.
16. Jian, Zhou, Luqing, Zhang, Fuchu, Dai (2013) "Numerical simulation of direct shear tests for rock and soil mixture in a landslide based on bonded-particle model," *Chinese Journal of Rock Mechanics and Engineering*, Vol 32 (supp), pp 2650-2660. (in Chinese)
17. Xiuli, Ding, Yaoxu, Li and Xin, Wang (2010) "Particle flow modeling mechanical properties of soil rock mixture based on digital image," *Chinese Journal of Rock Mechanics and Engineering*, Vol 29, No.3, pp477-484. (in Chinese)
18. Wenjie, Xu and Yonggang, Wang (2010) "Meso-structural permeability of S-RM based on numerical tests," *Chinese Journal of Geotechnical Engineering*, Vol 32, No.4, pp 542-550. (in Chinese)

